Beyond 5G Localization at mmWaves in 3GPP Urban Scenarios with Blockage Intelligence

(Invited Paper)

Gianluca Torsoli*, Moe Z. Win†, and Andrea Conti*

*Department of Engineering and CNIT, University of Ferrara, Via Saragat 1, 44122 Ferrara, Italy
(e-mail: gianluca.torsoli@unife.it, a.conti@ieee.org)

†Laboratory for Information and Decision Systems, Massachusetts Institute of Technology, Cambridge, MA 02139 USA
(e-mail: moewin@mit.edu)

2023 IEEE/ION Position, Location and Navigation Symposium (PLANS) | 978-1-6654-1772-3/23/$31.00 ©2023 IEEE | DOI: 10.1109/PLANS53410.2023.10140112

***Abstract*—Accurate positional information is crucial for numerous emerging applications in fifth generation (5G) and beyond wireless ecosystems. However, the localization requirements defined by the 3rd Generation Partnership Project (3GPP) are particularly challenging to achieve, especially in complex environments such as urban scenarios, due to non-line-of-sight conditions, outdoor-to-indoor penetration loss, and multipath propagation. Such effects are detrimental to localization accuracy, especially at mmWaves. This paper introduces the concept of blockage intelligence (BI) to provide a probabilistic representation of wireless propagation conditions. Such representation is then exploited in soft information (SI)-based localization to overcome the limitations of conventional localization approaches. Localization case studies are presented according to the 3GPP-standardized urban microcell (UMi) scenario at mmWaves with fully 3GPP-compliant simulations. Results show that BI together with SI-based localization is able to provide a significant performance gain with respect to existing techniques in 5G and beyond wireless networks.**

***Index Terms*—5G, localization, NLOS identification, 3GPP, wireless networks.**

I. Introduction

Location awareness [1] is fundamental to network orchestration and to enable a myriad of applications in fifth generation (5G) and beyond wireless networks [2], [3], including autonomous driving [4]–[6], smart environments [7]–[9], and Internet-of-Things (IoT) [10]–[12]. In particular, 5G and beyond wireless networks in urban environments can leverage accurate localization to provide several services, including support to first responders, traffic monitoring, and flow contol [13]. In this context, 3rd Generation Partnership Project (3GPP) study items for 5G Advanced (5GA) are putting an increasing emphasis on expanding and enhancing the localization capabilities of 5G networks [14], [15]. This can be accomplished by leveraging other improvements expected for 5GA, including the use of artificial intelligence and machine learning (ML) techniques as well as enhancements in the data collection [16], [17]. However, satisfying the key performance indicators levels required by 3GPP for localization accuarcy is particularly challenging. Urban scenarios are characterized by complex propagation conditions due to non-line-of-sight (NLOS) propagation, outdoor-to-indoor (O2I) penetration loss, and multipath propagation [18], [19]. Such impairments are detrimental to localization accuracy, especially at millimeter waves [20]. Therefore, enhanced localization techniques are needed to unleash the full potential of localization in 5G and beyond networks at mmWaves. In particular, NLOS identification techniques are expected to provide a great benefit to localization algorithms.

Exisiting approaches for NLOS identification exploit characteristics of the wireless environment to provide binary information on NLOS propagation conditions [21]–[23]. However, the binary information provided by existing NLOS identification is unable to represent the different conditions that may generate NLOS propagation. Moreover, several techniques for NLOS identification require a prior characterization of the wireless environment, which is not always available, especially in dynamic environments like urban scenarios.

The goal of this paper is to improve localization accuracy in complex wireless environments. We introduce the concept of blockage intelligence (BI) to overcome the limitations of existing NLOS identification [24]. The key idea is to leverage the rich information encapsulated in the received signals to provide a probabilistic characterization of the wireless channel conditions. The information provided by BI is therefore seamlessly integrated with the recently proposed soft information (SI)-based localization [25] to enhance location awareness in 5G and beyond wireless networks. We advocate the use of BI not only as a probabilistic NLOS identification, but also as an indicator of the quality of the wireless channel conditions.

This paper introduces the concept of BI to improve location awareness in complex urban wireless scenarios. The key contributions of this paper can be summarized as follows:

- introduction of the BI concept for providing a probabilistic characterization of wireless propagation conditions in urban scenarios; and
- quantification of the localization performance gain enabled by BI in the 3GPP-standardized urban microcell (UMi) scenario.

Authorized licensed use limited to: MIT Libraries. Downloaded on November 01,2023 at 19:09:36 UTC from IEEE Xplore. Restrictions apply.

The remainder of the paper is organized as follows. Section II briefly describes localization in 5G networks; Section III describes a method for obtaining BI; Section IV presents two case studies in the 3GPP-standardized UMi scenario; Finally, Section V provides our conclusions.

Notations: A random variable and its realization are denoted by x and x; a random vector and its realization are denoted by $\mathbf{x}$ and $\boldsymbol{x}$; a set is denoted by calligraphic fonts as $\mathcal{X}$. For a vector $\boldsymbol{x}$, its transpose is denoted by $\boldsymbol{x}^{\mathrm{T}}$. For a complex variable x, its conjugate is denoted by x^{*}. The smallest integer grater or equal to x is denoted by $\lceil x \rceil$. The function $f_{\mathbf{x}}(\boldsymbol{x};\boldsymbol{\theta})$ indicates the probability distribution function (PDF) of a continous random vector $\mathbf{x}$ parametrized by $\boldsymbol{\theta}$. $\mathbb{E}_{\mathsf{x}|\mathsf{y}}\{\cdot|\boldsymbol{y}\}$ denotes the expectation with respect to the random variable x conditional on $\mathbf{y} = \boldsymbol{y}$.

II. Localization in 5G networks

The goal of localization in 5G wireless networks is to estimate the position $\boldsymbol{p} \in \mathbb{R}^2$ of a user equipment (UE) based on the exchange of measurements with a set of nodes, namely gNodeBs (gNBs), with known positions and indexed by $j \in \mathcal{N}_{\mathrm{b}} = \{1, 2, \ldots, N_{\mathrm{b}}\}$, where N_{b} is the number of gNBs available for localization. 3GPP specifications define two reference signals (RSs) obtained via orthogonal frequency division multiplexing (OFDM) dedicated to localization, i.e., the positioning reference signal (PRS) for downlink (DL) localization and the sounding reference signal (SRS) for uplink (UL) localization [26]. The two reference signals can be transmitted in both frequency range 1 (FR1) (i.e., central frequency below 7.125 GHz) and frequency range 2 (FR2) (i.e., central frequency between 24.25 GHz and 52.6 GHz) with various time-frequency configurations [26]. According to 3GPP specifications [27], [28], the RSs can be transmitted and processed to extract single-value estimates (SVEs) which can be exploited to perform UE localization, including estimates of time difference-of-arrival (TDOA), round-trip time (RTT), and angle-of-departure (AOD).

A. Inference of SVEs

RTT and TDOA measurements are obtained based on time-of-arrival (TOA) measurements. In particular, a conventional approach for TOA estimation is based on the detection of the delay associated with the earliest peak in the magnitude of the cross-correlation between the transmitted and the received RS. In more detail, let $r[n]$ and $s[n]$ denote the sampled version of the received and of the transmitted RS, respectively. Then, the cross-correlation between $r[n]$ and $s[n]$ is given by

$$R[n] = \sum_{k=0}^{N_{\mathrm{s}}-1} r[n] s^{*}[n-k] \tag{1}$$

for $n = 0, 1, \ldots, N_{\mathrm{s}}-1$, where N_{s} is the number of samples in the received RS. To estimate the TOA, it is possible to proceed iteratively on (1), detecting at each iteration the strongest peak and then removing its contribution from the cross-correlation. After N_{I} iterations, where N_{I} is selected as the number of iterations that provide the minimum average ranging error, the TOA is estimated as the smallest delay detected during the iterative procedure [29]. Based on TOA estimations, the RTT is obtained as the two-way TOA, accounting for both DL and UL, while the TDOA is obtained subtracting the TOA of a reference gNB to the TOA obtained from all the other gNBs available for localization [30].

B. SI-based localization

SI-based localization has been recently proposed to overcome the limitations of existing localization algorithms. Specifically, SI-based localization leverages machine learning techniques to provide a statistical characterization of the relationship between UE position, measurements, and contextual information [25]. In paticular, SI is composed of soft feature information (SFI) and soft context information (SCI), which are exploited jointly for localization. Let $\boldsymbol{y}$ be a measurement obtained exchanging information with a gNB and let $\boldsymbol{\theta}$ be the positional feature associated with $\boldsymbol{y}$. Then, the corresponding SFI is given by

$$\mathcal{L}_{\boldsymbol{y}}(\boldsymbol{\theta}) \propto f_{\mathbf{y}}(\boldsymbol{y};\boldsymbol{\theta}). \tag{2}$$

For example, if $\boldsymbol{y}$ denotes an RTT measurement, the corresponding positional feature denotes the real distance between the gNB and the UE.[1] Given a collection of independent measurements obtained from different gNBs, and considering that no contextual information is available, the UE position can be determined as

$$\hat{\boldsymbol{p}} = \arg\max_{\tilde{\boldsymbol{p}}} \prod_{j \in \mathcal{N}_{\mathrm{b}}} \mathcal{L}_{\boldsymbol{y}_j}(\boldsymbol{\theta}_j(\tilde{\boldsymbol{p}})) \,. \tag{3}$$

The SFI is obtained as proportional to a generative model, which is an approximation of the joint probability distribution of measurements and positional features. The generative model can be estimated in complex wireless scenarios fitting a Gaussian mixture model (GMM) to a training dataset using the expectation-maximization algorithm [31].

III. Blockage Intelligence

Localization algorithms greatly benefit from the information provided by NLOS identification. However, existing NLOS identification techniques are binary, which makes the localization algorithms unable to effectively account for the different wireless propagation situations generated by NLOS conditions.

A. Feature extraction

To overcome the limitations of existing NLOS identification techniques, the key idea of BI is to leverage the rich information encapsulated in 5G received signals, and specifically in the cross-correlation (1) between the transmitted and the received RS. On the one hand, such cross-correlation encapsulates rich information on the wireless channel conditions. On the other hand, it is commonly available to localization algorithms as it is necessary for TOA estimation [32], [33]. In particular, only the absolute value of (1) is exploited for BI, which is

$$g[n] = |R[n]| \tag{4}$$

[1] Note that in such case both $\boldsymbol{y}$ and $\boldsymbol{\theta}$ are scalar values.

Authorized licensed use limited to: MIT Libraries. Downloaded on November 01,2023 at 19:09:36 UTC from IEEE Xplore. Restrictions apply.

TABLE I
STATISTICAL FEATURES USED FOR BI

Amplitude-based features	Time-based features
$\mu_\mathrm{a} = \frac{1}{N_\mathrm{c}} \sum_{m=0}^{N_\mathrm{c}-1} g[m]$	$\mu_\mathrm{t} = \sum_{m=0}^{N_\mathrm{c}-1} m\, T_\mathrm{s}\, \breve{g}[m]$
$\sigma_\mathrm{a}^2 = \frac{1}{N_\mathrm{c}} \sum_{m=0}^{N_\mathrm{c}-1} (g[m]-\mu_\mathrm{a})^2$	$\sigma_\mathrm{t}^2 = \sum_{m=0}^{N_\mathrm{c}-1} (mT_\mathrm{s}-\mu_\mathrm{t})^2\, \breve{g}[m]$
$\kappa_\mathrm{a} = \frac{1}{N_\mathrm{c}} \frac{\sum_{m=0}^{N_\mathrm{c}-1}(g[m]-\mu_\mathrm{a})^4}{(\sigma_\mathrm{a}^2)^2}$	$\kappa_\mathrm{t} = \frac{\sum_{m=0}^{N_\mathrm{c}-1}(mT_\mathrm{s}-\mu_\mathrm{t})^4\, \breve{g}[m]}{(\sigma_\mathrm{t}^2)^2}$
$\chi_\mathrm{a} = \frac{1}{N_\mathrm{c}} \frac{\sum_{m=0}^{N_\mathrm{c}-1}(g[m]-\mu_\mathrm{a})^3}{(\sigma_\mathrm{a}^2)^{\frac{3}{2}}}$	$\chi_\mathrm{t} = \frac{\sum_{m=0}^{N_\mathrm{c}-1}(mT_\mathrm{s}-\mu_\mathrm{t})^3\, \breve{g}[m]}{(\sigma_\mathrm{t}^2)^{\frac{3}{2}}}$
$E = \sum_{m=0}^{N_\mathrm{c}-1} g[m]^2$	
$M = \max_m g[m]$	

for $n = 0, 1, \ldots, N_\mathrm{c}-1$ where $N_\mathrm{c} = \lceil T_\mathrm{m}/T_\mathrm{s} \rceil$, T_s is the RS sampling time, and T_m is the maximum path delay such that the received waveform contains positional information. The value of T_m is selected empirically based on the characteristics of the wireless scenario. However, $g[n]$ can have high dimensionality, especially when the RSs are transmitted at mmWaves, and a dimensionality reduction is needed to improve BI efficiency. We propose the use of a set of statistical features able to capture relevant information on amplitude and time dispersions of $g[n]$. The proposed set of features include mean μ, variance σ^2, kurtosis κ, and skewness χ of both the amplitude and the time dispersion of $g[n]$. In addition, also the energy E and the maximum value M of $g[n]$ are considered. The expressions of the features used for BI are reported in Table I, where

$$\breve{g}[n] = \frac{g[n]}{\sum_{m=0}^{N_\mathrm{c}-1} g[m]}\,. \tag{5}$$

B. Blockage intelligence model

The rich information obtained from the aforementioned statistical features is exploited to provide a probabilistic characterization of NLOS propagation conditions. In particular, the problem of determining the probability of NLOS can be formalized as a two-class supervised classification problem [36], [37]. Let $\mathsf{\gamma} \in \{+1, -1\}$ be a binary random variable that takes value $+1$ and -1 for NLOS and LOS propagation conditions, respectively, and let $\boldsymbol{\mathsf{v}} = [\mathsf{\mu}_\mathrm{a}, \mathsf{\sigma}_\mathrm{a}^2, \mathsf{\kappa}_\mathrm{a}, \mathsf{\chi}_\mathrm{a}, \mathsf{E}, \mathsf{M}, \mathsf{\mu}_\mathrm{t}, \mathsf{\sigma}_\mathrm{t}^2, \mathsf{\kappa}_\mathrm{t}, \mathsf{\chi}_\mathrm{t}]$ be a random vector containing the estimators for the statistical features in Table I. By considering an exponential loss function, a model $c(\boldsymbol{\nu})$ for NLOS classification is obtained as

$$c(\boldsymbol{\nu}) = \arg\min_{\breve{c}\,:\,\mathbb{R}^d \to \mathbb{R}} \mathbb{E}_{\mathsf{\gamma}|\boldsymbol{\mathsf{v}}}\{e^{-\mathsf{\gamma}\breve{c}(\boldsymbol{\mathsf{v}})} \mid \boldsymbol{\nu}\}\,. \tag{6}$$

Such approach for obtaining $c(\boldsymbol{\nu})$ is referred to as risk minimization and entails the determination of a function that maps a d-dimensional vector of statistical features extracted from the received RS to a value in $\mathbb{R}$ which is used for classification. In particular, equation (6) has a closed-form solution [36] given by

$$c(\boldsymbol{\nu}) = \frac{1}{2}\log\left(\frac{\mathbb{P}\{\mathsf{\gamma}=+1 \mid \boldsymbol{\nu}\}}{1-\mathbb{P}\{\mathsf{\gamma}=+1 \mid \boldsymbol{\nu}\}}\right) \tag{7}$$

leading to

$$\psi(\boldsymbol{\nu}) = \mathbb{P}\{\mathsf{\gamma}=+1 \mid \boldsymbol{\nu}\} = \frac{e^{c(\boldsymbol{\nu})}}{e^{-c(\boldsymbol{\nu})}+e^{c(\boldsymbol{\nu})}} \tag{8}$$

which is the NLOS probability given the set of statistical features extracted from (1), i.e., the equation needed for BI. However, since the joint probability distribution of $\mathsf{\gamma}$ and $\boldsymbol{\mathsf{v}}$ is not known a priori, $c(\boldsymbol{\nu})$ cannot be obtained in closed-form solving the risk minimization problem in (6). Therefore, it is necessary to obtain an approximation of $c(\boldsymbol{\nu})$ via empirical risk minimization (ERM) exploiting a training dataset $\mathcal{D} = \{(\boldsymbol{\nu}_n, \gamma_n)\}_{n=1}^{N_\mathrm{d}}$, where N_d denotes the number of training samples [37]. In particular, the choice of an exponential loss function enables efficient ERM via the Real AdaBoost algorithm [38]. Such algorithm leverages the training data to

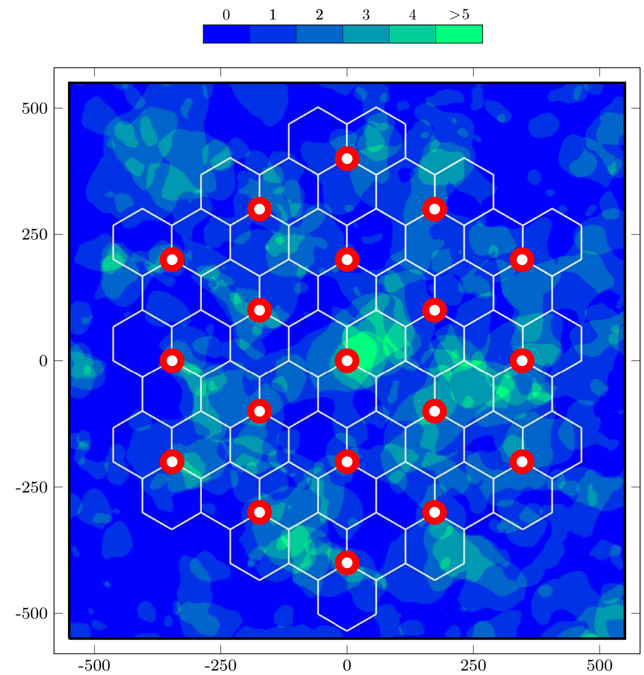

Fig. 1. Layout of the 3GPP UMi scenario. The red annuluses denote the gNBs location. The background of the figure is an example instantiation of the number of LOS gNBs for each point of the scenario. The coordinates on the axis are in meters.

Authorized licensed use limited to: MIT Libraries. Downloaded on November 01,2023 at 19:09:36 UTC from IEEE Xplore. Restrictions apply.

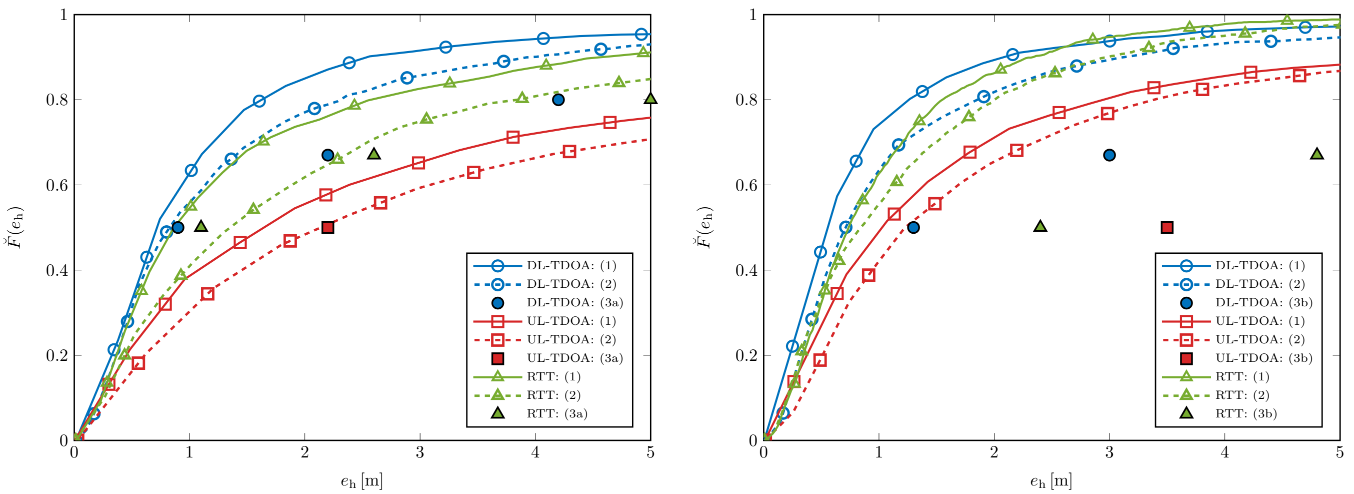

(a) Power boosting disabled

(b) Power boosting enabled

Fig. 2. ECDF of the horizontal localization error in the 3GPP UMi scenario at 30 GHz for (a) RS transmission without PB; and (b) RS transmission with PB. The localization performance are reported for (1) SI-based localization with BI; (2) SI-based localization without BI; (3a) results in [34]; and (3b) results in [35].

combine several classifiers with high-bias and low-variance (typically one-level decision trees [39]) to obtain an additive model which approximates $c(\boldsymbol{\nu})$ up to a constant factor which does not affect (8).

C. Blockage intelligence in SI-based localization

The integration of existing binary NLOS identification techniques in SI-based localization relies on determining two different generative models, tailored to NLOS and LOS propagation conditions [25]. However, the performance of SI-based localization would benefit from the integration of the probabilistic NLOS information provided by BI. On the one hand, the conventional binary information is not able to account for the different wireless propagation situations that may generate NLOS conditions. On the other hand, errors in NLOS identification may generate significative localization errors since the generative models are specific to the propagation conditions. To mitigate these challenges, we propose the direct integration of the probabilistic information provided by BI in the measurement vector used for SI-based localization, i.e., $\boldsymbol{y}' = [\boldsymbol{y}, \psi(\boldsymbol{\nu})]$. This enables to describe a wide variety of wireless propagation conditions in the SI-based localization model, leveraging the rich positional information provided by BI.

IV. Case Studies

This section analyzes and compares the performance gain offered by SI-based localization with BI in urban scenarios. In particular, performance is quantified in the 3GPP-standardized UMi scenario at mmWaves [18]. Fig. 1 shows the layout of the UMi scenario, which is composed of 19 gNBs with three antenna sector for each gNB. The localization performance is evaluated in FR2, i.e., where the effect of NLOS conditions is more critical. Specifically, the PRS and the SRS are transmitted with a central frequency of 30 GHz and a bandwidth of 400 MHz. According to 3GPP specifications, it is possible to enable power boosting on the PRS and SRS to improve the localization performance [26]. In the following, localization results are therefore reported considering the RSs transmission with and without power boosting. Specifically, the power boosting level is set equal to 7.78 dB and 6.02 dB for PRS and SRS transmission, respectively [28]. Results are obtained in full compliance with 3GPP technical reports. Specifically, the RSs are generated according to the specifications in [26], [28], and the gNBs and UEs characteristics are set according to [18]. The wireless channels are generated as in [18] via the QuaDriGa channel simulator [40].

To quantify the localization performance, 200 instantiations of the UMi scenarios with spatially consistent wireless channels and NLOS conditions were generated. For each of them, 10 UEs were deployed in the scenario with random positions and orientations. The SVEs considered for localization are DL-TDOA, UL-TDOA, and RTT, as in 3GPP technical reports [28]. Moreover, if BI is employed for localization, the reference gNB for TDOA measurements is selected through BI as the gNB which provides the lowest NLOS probability, otherwise, it is selected as the gNB which provides the maximum reference signal received power (RSRP). The data are divided through 10-fold cross-validation [31]. The 70% of the training data are used for training BI as in Sec. III and for determining the number of iterations N_{I} the minimizes the TOA estimation error in the ranging algorithm as in Sec. II-A. The remaining 30% of the training data are used for training the generative model for SI-based localization, which consists of a GMM with 12 components. Results are reported in terms of the ECDF $\breve{F}(e_{\mathrm{h}})$ of the horizontal localization error e_{h} for

Authorized licensed use limited to: MIT Libraries. Downloaded on November 01,2023 at 19:09:36 UTC from IEEE Xplore. Restrictions apply.

TABLE II
LOCALIZATION ERROR PERCENTILES
WITHOUT POWER BOOSTING

Configuration	Percentile			
	50th	67th	80th	90th
DL-TDOA: [34]	0.90 m	2.20 m	4.20 m	9.40 m
DL-TDOA: SI	0.81 m	1.36 m	2.27 m	4.00 m
DL-TDOA: SI+BI	0.73 m	1.09 m	1.46 m	2.54 m
UL-TDOA: [34]	2.20 m	6.20 m	16.80 m	95.30 m
UL-TDOA: SI	2.36 m	4.12 m	8.84 m	64.29 m
UL-TDOA: SI+BI	1.42 m	3.33 m	7.14 m	45.96 m
RTT: [34]	1.10 m	2.60 m	5.00 m	11.60 m
RTT: SI	1.27 m	2.30 m	3.83 m	7.15 m
RTT: SI+BI	0.84 m	1.47 m	2.53 m	4.63 m

TABLE III
LOCALIZATION ERROR PERCENTILES
WITH POWER BOOSTING

Configuration	Percentile			
	50th	67th	80th	90th
DL-TDOA: [35]	1.30 m	3.00 m	5.70 m	9.70 m
DL-TDOA: SI	0.76 m	1.15 m	1.79 m	3.07 m
DL-TDOA: SI+BI	0.62 m	0.94 m	1.56 m	2.19 m
UL-TDOA: [35]	3.50 m	6.30 m	11.10 m	18.30 m
UL-TDOA: SI	1.21 m	2.18 m	3.39 m	7.02 m
UL-TDOA: SI+BI	1.04 m	1.73 m	2.77 m	5.89 m
RTT: [35]	2.40 m	4.80 m	8.20 m	12.70 m
RTT: SI	0.83 m	1.37 m	1.99 m	2.97 m
RTT: SI+BI	0.73 m	1.10 m	1.54 m	2.33 m

SI-based localization with and without BI. In addition, such localization performance is compared with results in 3GPP technical reports [28]. Specifically, the results considered are the ones reported in [34] and in [35] for localization without and with power boosting, respectively.

A. Results in 3GPP UMi scenario without power boosting

Fig. 2a shows the ECDF of the horizonal localization error for RSs transmission at 30 GHz without power boosting. In addition, the most significant localization error percentiles are reported in Table II. It can be observed that the use of SI-based localization with BI provides a significant localization accuracy improvement with respect to both SI-based localization without BI and results in 3GPP technical reports [34]. In particular, considering DL-TDOA measurements, the localization performance gain at the 90th percentile is equal to 1.46 m and 6.86 m with respect to SI-based localization without BI and results in [34], respectively. An even larger gain is obtained considering localization based on RTT measurements. Specifically, at the 90th percentile, the localization error of SI-based localization with BI is equal to 4.63 m, which consists in a significant improvement compared to the 7.15 m achieved by SI-based localization without BI and the 11.60 m reported in [34]. Finally, it can be observed that despite the significant gain provided by BI with respect to other techniques for localization with UL-TDOA, the localization performance remains unsatisfactory. This is because the transmitted power for UL localization in UMi scenario at mmWaves without power boosting is not sufficient to obtain reliable UL-TDOA measurements.

B. Results in 3GPP UMi scenario with power boosting

Fig. 2b shows the ECDF of the horizonal localization error for RSs transmission at 30 GHz without power boosting. In addition, the most significant localization error percentiles are reported in Table III. It can be observed that localization using SI-based localization with BI via DL-TDOA measurements enables sub-meter localization accuracy at the 67th percentile and an accuracy of around 2.20 m at the 90th percentile. This represents a gain of around 1 m with respect to SI-based localization without BI and larger than 7 m if compared to results in [35]. Similar localization accuracies are obtained for localization with RTT measurements. In particular, SI-based localization with BI enables a localization performance gain at the 90th percentile of more than 10 m with respect to results in [35]. Finally, the use of power boosting enables efficient localization with UL-TDOA measurements. Specifically, SI-based localization with BI provides a localization accuracy of 5.89 m at the 90th percentile, which represents a significant performance gain with respect to the 7.02 m achieved by SI-based localization without BI and the 18.30 m reported in [35].

V. CONCLUSION

This paper introduced the concept of blockage intelligence (BI) to provide a probabilistic representation of wireless propagation conditions in fifth generation (5G) and beyond wireless networks. This is obtained by leveraging the rich positional information encapsulated in the cross-correlation between the transmitted and received reference signals (RSs). Results show that the knowledge of information on wireless channel propagation conditions is vital to enhance the performance of localization algorithms, especially for location awareness in complex wireless scenarios. In particular, the use of BI together with soft information (SI)-based localization in 3rd Generation Partnership Project (3GPP) urban microcell (UMi) scenarios at mmWaves enables a significant performance gain with respect to the localization performance reported in 3GPP technical reports. The proposed approach represents a step towards fulfilling the localization service level requirements expected for 5G and beyond wireless networks.

ACKNOWLEDGMENT

The fundamental research described in this paper was supported, in part, by the Office of Naval Research under Grant N62909-22-1-2009, by the National Science Foundation under Grant CNS-2148251, and by funds from federal agency and industry partners in the RINGS program.

Authorized licensed use limited to: MIT Libraries. Downloaded on November 01,2023 at 19:09:36 UTC from IEEE Xplore. Restrictions apply.

References

[1] M. Z. Win *et al.*, "Network localization and navigation via cooperation," *IEEE Commun. Mag.*, vol. 49, no. 5, pp. 56–62, May 2011.

[2] A. Conti *et al.*, "Location awareness in beyond 5G networks," *IEEE Commun. Mag.*, vol. 59, no. 11, pp. 22–27, Nov. 2021.

[3] S. Dwivedi *et al.*, "Positioning in 5G networks," *IEEE Commun. Mag.*, vol. 59, no. 11, pp. 38–44, Nov. 2021.

[4] A. Bazzi, A. O. Berthet, C. Campolo, B. M. Masini, A. Molinaro, and A. Zanella, "On the design of sidelink for cellular V2X: A literature review and outlook for future," *IEEE Access*, vol. 9, pp. 97 953–97 980, 2021.

[5] J. Thomas, J. Welde, G. Loianno, K. Daniilidis, and V. Kumar, "Autonomous flight for detection, localization, and tracking of moving targets with a small quadrotor," *IEEE Robot. Autom. Lett.*, vol. 2, no. 3, pp. 1762–1769, Jul. 2017.

[6] R. Karlsson and F. Gustafsson, "The future of automotive localization algorithms: Available, reliable, and scalable localization: Anywhere and anytime," *IEEE Signal Process. Mag.*, vol. 34, no. 2, pp. 60–69, Mar. 2017.

[7] G. Cardone *et al.*, "Fostering participaction in smart cities: a geo-social crowdsensing platform," *IEEE Commun. Mag.*, vol. 51, no. 6, pp. 112–119, Jun. 2013.

[8] A. Zanella, N. Bui, A. Castellani, L. Vangelista, and M. Zorzi, "Internet of things for smart cities," *IEEE Internet of Things J.*, vol. 1, no. 1, pp. 22–32, Feb. 2014.

[9] Y. Gu, Y. Kamiya, and S. Kamijo, "Integration of positioning and activity context information for lifelog in urban city area," *NAVIGATION*, vol. 67, pp. 163–179, 2020.

[10] S. D'oro, L. Galluccio, G. Morabito, and S. Palazzo, "Exploiting object group localization in the Internet of Things: Performance analysis," *IEEE Trans. Veh. Technol.*, vol. 64, no. 8, pp. 3645–3656, Aug. 2015.

[11] F. Zabini and A. Conti, "Inhomogeneous Poisson sampling of finite-energy signals with uncertainties in $\mathbb{R}^d$," *IEEE Trans. Signal Process.*, vol. 64, no. 18, pp. 4679–4694, Sep. 2016.

[12] S. G. Nagarajan, P. Zhang, and I. Nevat, "Geo-spatial location estimation for Internet of Things (IoT) networks with one-way time-of-arrival via stochastic censoring," *IEEE Internet Things J.*, vol. 4, no. 1, pp. 205–214, Feb. 2017.

[13] *Technical Specification Group Radio Access Network; Technical Specification Group Services and System Aspects; Study on positioning use cases*, 3GPP™ Std. TR 22.872 V16.1.0, Sept. 2018, Release 16.

[14] *Technical Specification Group Radio Access Network; Study on expanded and improved NR positioning*, 3GPP™ Std. TR 38.859 V1.0.0, Dec. 2022, Release 18.

[15] X. Lin, "An overview of 5G advanced evolution in 3GPP Release 18," *IEEE Commun. Stand. Mag.*, vol. 6, no. 3, pp. 77–83, 2022.

[16] *Technical Specification Group Radio Access Network; Study on Artificial Intelligence (AI)/Machine Learning (ML) for NR air interface*, 3rd Generation Partnership Project 3GPP™ TR 38.843 V18.0.0, 2022, Release 18.

[17] *Technical Specification Group Radio Access Network; Evolved Universal Terrestrial Radio Access (E-UTRA) and NR; Study on enhancement for Data Collection for NR and EN-DC*, 3rd Generation Partnership Project 3GPP™ TR 37.817 V17.0.0, Apr. 2022, Release 17.

[18] *Technical Specification Group Radio Access Network; Study on channel model for frequencies from 0.5 to 100 GHz*, 3rd Generation Partnership Project 3GPP™ TR 38.901 V17.0.0, Mar. 2022, Release 17.

[19] K. Haneda *et al.*, "5G 3GPP-like channel models for outdoor urban microcellular and macrocellular environments," in *Proc. IEEE Semiannual Veh. Technol. Conf.*, Nanjing, China, May 2016, pp. 1–7.

[20] S. Rangan, T. S. Rappaport, and E. Erkip, "Millimeter-wave cellular wireless networks: Potentials and challenges," *Proc. IEEE*, vol. 102, no. 3, pp. 366–385, 2014.

[21] A. Conti, M. Guerra, D. Dardari, N. Decarli, and M. Z. Win, "Network experimentation for cooperative localization," *IEEE J. Sel. Areas Commun.*, vol. 30, no. 2, pp. 467–475, Feb. 2012.

[22] B. Silva and G. P. Hancke, "IR-UWB-based non-line-of-sight identification in harsh environments: Principles and challenges," *IEEE Trans. Ind. Informat.*, vol. 12, no. 3, pp. 1188–1195, Jun. 2016.

[23] K. Yu, K. Wen, Y. Li, S. Zhang, and K. Zhang, "A novel NLOS mitigation algorithm for UWB localization in harsh indoor environments," *IEEE Trans. Veh. Technol.*, vol. 68, no. 1, pp. 686–699, Jan. 2019.

[24] G. Torsoli, M. Z. Win, and A. Conti, "Blockage intelligence in complex environments for beyond 5G localization," *IEEE J. Sel. Areas Commun.*, pp. 1–14, Third quarter 2023, special issue on *3GPP Technologies: 5G-Advanced and Beyond*, to appear.

[25] A. Conti, S. Mazuelas, S. Bartoletti, W. C. Lindsey, and M. Z. Win, "Soft information for localization-of-things," *Proc. IEEE*, vol. 107, no. 11, pp. 2240–2264, Nov. 2019.

[26] *Technical Specification Group Radio Access Network; NR; Physical channels and modulation*, 3GPP™ Std. TS 38.211 V16.6.0, Jun. 2021, Release 16.

[27] *Technical Specification Group Radio Access Network; NG Radio Access Network (NG-RAN); Stage 2 functional specification of User Equipment (UE) positioning in NG-RAN*, 3GPP™ Std. TS 38.305 V17.0.0, Mar. 2022, Release 17.

[28] *Technical Specification Group Radio Access Network; Study on NR positioning support*, 3GPP™ Std. TR 38.855 V16.0.0, Mar. 2019, Release 16.

[29] H. Ryden, A. A. Zaidi, S. M. Razavi, F. Gunnarsson, and I. Siomina, "Enhanced time of arrival estimation and quantization for positioning in LTE networks," in *Proc. IEEE 27th Int. Symp. Pers., Indoor, Mobile Radio Commun (PIMRC)*, Valencia, Spain, 2016, pp. 1–6.

[30] G. Torsoli, M. Z. Win, and A. Conti, "Selection of reference base station for TDOA-based localization in 5G and beyond IIoT," in *Proc. IEEE Global Telecomm. Conf.*, Rio de Janeiro, Brazil, Dec. 2022, pp. 317–322.

[31] C. M. Bishop, *Pattern Recognition and Machine Learning*. New York, NY, USA: Springer, 2006.

[32] I. Guvenc and C.-C. Chong, "A survey on TOA based wireless localization and NLOS mitigation techniques," *IEEE Commun. Surveys Tuts.*, vol. 11, no. 3, pp. 107–124, 2009.

[33] P. Wang and Y. Morton, "Performance comparison of time-of-arrival estimation techniques for LTE signals in realistic multipath propagation channels," *NAVIGATION*, vol. 67, pp. 691–712, 2020.

[34] "R1-1903021: Evaluation results for RAT-dependent positioning techniques," 3GPP TSG-RAN WG1 meeting #96, Qualcomm, Mar. 2019.

[35] "R1-1901577: Performance evaluation of NR positioning," 3GPP TSG-RAN WG1 meeting #96, Huawei, Mar. 2019.

[36] T. Hastie, R. Tibshirani, and J. Friedman, *The Elements of Statistical Learning*, 2nd ed. New York, NY: Springer, 2009.

[37] V. Vapnik, "Principles of risk minimization for learning theory," in *Proc. 4th International Conference on Neural Information Processing Systems*, San Francisco, CA, USA, 1991, p. 831–838.

[38] J. Friedman, T. Hastie, and R. Tibshirani, "Additive logistic regression: A statistical view of boosting," *The Annals of Statistics*, vol. 28, pp. 337–407, Apr. 2000.

[39] L. Breiman, J. Friedman, R. A. Olshen, and C. J. Stone, *Classification and Regression Trees*. Wadsworth Publishing Company, 1984.

[40] S. Jaeckel, L. Raschkowski, K. Börner, and L. Thiele, "QuaDRiGa: A 3-D multi-cell channel model with time evolution for enabling virtual field trials," *IEEE Trans. Antennas Propag.*, vol. 62, no. 6, pp. 3242–3256, Jun. 2014.

Authorized licensed use limited to: MIT Libraries. Downloaded on November 01,2023 at 19:09:36 UTC from IEEE Xplore. Restrictions apply.